

Lubricin Restoration in a Mouse Model of Congenital Deficiency

Adele Hill,¹ Kimberly A. Waller,² Yajun Cui,³ Justin M. Allen,¹ Patrick Smits,³
Ling X. Zhang,² Ugur M. Ayturk,¹ Steven Hann,³ Samantha G. Lessard,³
David Zurakowski,³ Matthew L. Warman,⁴ and Gregory D. Jay⁵

Objective. Congenital deficiency of the principal boundary lubricant in cartilage (i.e., lubricin, encoded by the gene *PRG4*) increases joint friction and causes progressive joint failure. This study was undertaken to determine whether restoring lubricin expression in a mouse model would prevent, delay, or reverse the disease process caused by congenital deficiency.

Methods. Using genetically engineered lubricin-deficient mice, we restored gene function before conception or at ages 3 weeks, 2 months, or 6 months after birth. The effect of restoring gene function (i.e., expression of lubricin) on the tibiofemoral patellar joints of mice was evaluated histologically and by ex vivo biomechanical testing.

Results. Restoring gene function in mice prior to conception prevented joint disease. In 3-week-old mice, restoring gene function improved, but did not normalize, histologic features of the articular cartilage and whole-joint friction. In addition, cyclic loading of the joints produced fewer activated caspase 3–containing chondrocytes when lubricin expression was restored, as compared to that in littermate mice whose gene function was not restored (nonrestored controls). Restoration of lubricin expression in 2-month-old or 6-month-old mice had no beneficial effect on histopathologic cartilage damage, extent of whole-joint friction, or activation of caspase 3 when compared to nonrestored controls.

Conclusion. When boundary lubrication is congenitally deficient and cartilage becomes damaged, the window of opportunity for restoring lubrication and slowing disease progression is limited.

In order to develop successful strategies for treating disease, it is important to know whether and when features of disease can be prevented, delayed, or reversed. These considerations are relevant in the management of patients with congenital and acquired joint diseases. For example, nearly 50% of individuals with anterior cruciate ligament (ACL) injuries will develop signs and symptoms of arthritis within 15 years following their injury, independent of whether the injured joint has been surgically stabilized (1). This observation suggests that either it is not possible to prevent progressive joint damage following many ACL injuries or current treatment strategies are inadequate. Determining whether joint damage can be prevented or reversed, and identifying critical windows of opportunity for doing so, will be essential for providing optimal care and controlling health care costs.

Insights into processes involved in joint injury and repair may come from the study of patients with the auto-

Supported by the NIH (grant AR-050180).

¹Adele Hill, PhD, Justin M. Allen, PhD, Ugur M. Ayturk, PhD: Boston Children's Hospital and Harvard Medical School, Boston, Massachusetts; ²Kimberly A. Waller, PhD, Ling X. Zhang, MD: Alpert Medical School of Brown University and Rhode Island Hospital, Providence; ³Yajun Cui, PhD, DMD, Patrick Smits, PhD, Steven Hann, PhD, Samantha G. Lessard, BA, David Zurakowski, PhD: Boston Children's Hospital, Boston, Massachusetts; ⁴Matthew L. Warman, MD: Howard Hughes Medical Institute, Boston Children's Hospital, and Harvard Medical School, Boston, Massachusetts; ⁵Gregory D. Jay, MD, PhD: Rhode Island Hospital, Alpert Medical School of Brown University, and Brown University School of Engineering, Providence, Rhode Island.

Drs. Hill and Waller contributed equally to this work.

Drs. Cui, Warman, and Jay receive royalties for antilubricin antibodies licensed by Millipore. Dr. Jay holds a patent related to tribonection polypeptides and the therapeutic use of lubricin in joints, and has received a Phase II Small Business Technology Transfer award to explore the commercialization of intraarticular lubricin injections through clinical translation efforts related to the patent.

Address correspondence to Matthew L. Warman, MD, Boston Children's Hospital, Departments of Orthopaedic Surgery and Genetics, Enders 260, 320 Longwood Avenue, Boston MA 02115 (e-mail: matthew.warman@childrens.harvard.edu); or to Gregory D. Jay, MD, PhD, Rhode Island Hospital, Department of Emergency Medicine, One Hoppin Street, Suite 106, Providence, RI 02917 (e-mail: gregory_jay_MD@brown.edu).

Submitted for publication September 12, 2014; accepted in revised form July 2, 2015.

somal recessive disease camptodactyly–arthropathy–coxa vara–pericarditis (CACP) syndrome and from animal models of this disease. CACP is a precocious joint failure disorder caused by genetic deficiency of lubricin (encoded by *PRG4*) (2), the major boundary lubricant in articulating joints (3). During development, lubricin is expressed by surface chondrocytes as soon as the joint cavitates (4). Subsequently, superficial zone chondrocytes and type B synoviocytes continue to express lubricin throughout life (4,5). In patients with congenital (i.e., CACP) or acquired (e.g., inflammatory arthritis) deficiencies of lubricin, the synovial fluid fails to reduce friction in the boundary mode (6).

Lubricin-knockout (*Prg4*^{-/-}) mice recapitulate some of the disease features observed in patients with CACP, such as noninflammatory synovial hyperplasia and precocious cartilage failure (4,6). Importantly, damage to the cartilage surface in lubricin-knockout mice is detectable by age 2 weeks, and a significant increase in whole-joint friction is evident by age 2 months (7). Thus, congenital absence of lubricin damages the cartilage surface and alters whole-joint mechanics early in life. However, complete cartilage failure can take a year to develop in *Prg4*^{-/-} mice and decades to develop in patients with CACP (8). Therefore, despite the absence of adequate boundary lubrication and the rapid appearance of joint damage, the progression to joint failure occurs at a much slower rate. This raises the possibility that any incipient traumatic event, such as ACL or meniscal injury, that causes cartilage surface damage will inevitably progress to cartilage failure over the long term (9).

To determine whether the cartilage damage that results from congenital lubricin deficiency is treatable, we restored endogenous lubricin expression postnatally in lubricin-knockout mice. We created a strain of mice that have a reversible gene-trap (GT) in *Prg4*. This gene-trap blocks lubricin expression; thus, upon Cre-mediated excision of the gene-trap, lubricin expression is restored. We restored lubricin expression in mice prior to conception or at ages 3 weeks, 2 months, or 6 months after birth, and evaluated the histologic features of the articular cartilage and the extent of whole-joint friction in these mice, compared to littermate mice whose gene function was not restored (nonrestored controls).

MATERIALS AND METHODS

Animal models. All animal studies were performed with the approval of the Institutional Animal Care and Use Committees at Boston Children's Hospital and Rhode Island Hospital.

Mice that are homozygous (*Prg4*^{-/-}) or heterozygous (*Prg4*^{+/-}) for lubricin loss-of-function alleles have been described previously (4). We generated mice with a new *Prg4* allele (*Prg4*^{GT}) (stock no. 025740; The Jackson Laboratory) (Figure 1). The *Prg4*^{GT} allele was created by homologous recombination in 129/SvEv ES cells (Figure 1A). The gene-trap, which consists of a loxP-flanked artificial exon that contains a strong splice acceptor, a LacZ-coding sequence that is "in frame" with *Prg4*, an internal ribosome entry site, a reverse tetracycline *trans*-activator (rtTA) cassette, a polyadenylation site, and a neomycin selection cassette driven by its own promoter, was derived from the gene-trap secretory vector pTT1TM (10). The *Prg4*^{GT} allele is designed to produce membrane-anchored β -galactosidase and rtTA, instead of lubricin, in cells in which *Prg4* is normally expressed.

The artificial exon can be excised with Cre-recombinase (i.e., *Prg4*^{GT^R}) to restore lubricin expression. We used 2 different Cre-recombinase alleles to excise the gene-trap. One allele, Tg(*eIIx*-Cre) (stock no. 003724; The Jackson Laboratory), excises the gene-trap in the germline. The other allele, *ROSA26*^{CreERT2} (stock no. 008463; The Jackson Laboratory), causes widespread excision of the gene-trap after injection of tamoxifen.

Standard animal husbandry was performed to generate cohorts of male and female mice. These mice, all on mixed B6/129 genetic backgrounds, had one of the following genotypes: *Prg4*^{-/-}, *Prg4*^{+/-}, *Prg4*^{GT/GT}, *Prg4*^{GT/+}, *Prg4*^{GT/-}, *Prg4*^{GT^R/GT}, *ROSA26*^{CreERT2/+}, *Prg4*^{GT/+}; *ROSA26*^{CreERT2/+}, *Prg4*^{GT^R/-}, and *Prg4*^{GT^R/GT}.

Induction of Cre-mediated recombination using tamoxifen. Mice with the genotypes *Prg4*^{GT/+}, *Prg4*^{GT/GT}, and *Prg4*^{GT^R/GT}; *ROSA26*^{CreERT2/+} were given daily intraperitoneal injections of tamoxifen dissolved in corn oil (Sigma-Aldrich) at a dose of 0.1 mg/gm body weight for 10 consecutive days, beginning at ages 3 weeks, 2 months, or 6 months. The mice were then permitted to age normally until they were killed with CO₂ inhalation.

Sample collection and processing. The joints of mice were removed postmortem and processed immediately thereafter. Samples of the cartilage tissue for knee joint histology were fixed in 4% (weight/volume) paraformaldehyde (PFA) in phosphate buffered saline (PBS) overnight, and then rinsed several times in PBS and decalcified with either EDTA in PBS (14% w/v, pH 7.4) for ~2 weeks or a mild formic acid decalcifier (Immunocal; Decal) for 12 hours. Decalcified samples were again washed in PBS, and then dehydrated through a graded PBS–ethanol series, incubated in xylene, bisected in the sagittal plane with a razor, and infiltrated with paraffin. Sagittal sections (6 or 8 μ m in thickness) were collected from the center of the bisected joint outward until the cruciate ligaments were no longer present, the tibial plateau became flattened, and the anterior and posterior portions of the meniscus were seen. Sections were stained with hematoxylin and eosin (H&E) in accordance with standard procedures (11).

Samples for X-Gal staining were fixed briefly with 0.2% glutaraldehyde, 5 mM EDTA, and 2 mM MgCl₂ in PBS. The samples were then rinsed in PBS containing 2 mM MgCl₂ and 0.02% Nonidet P40. X-Gal staining was performed overnight in the dark with constant shaking in X-Gal staining solution (2 mg/ml X-Gal, 5 mM potassium ferrocyanide, 5 mM potassium ferricyanide, 2 mM MgCl₂, and 0.02% Nonidet P40).

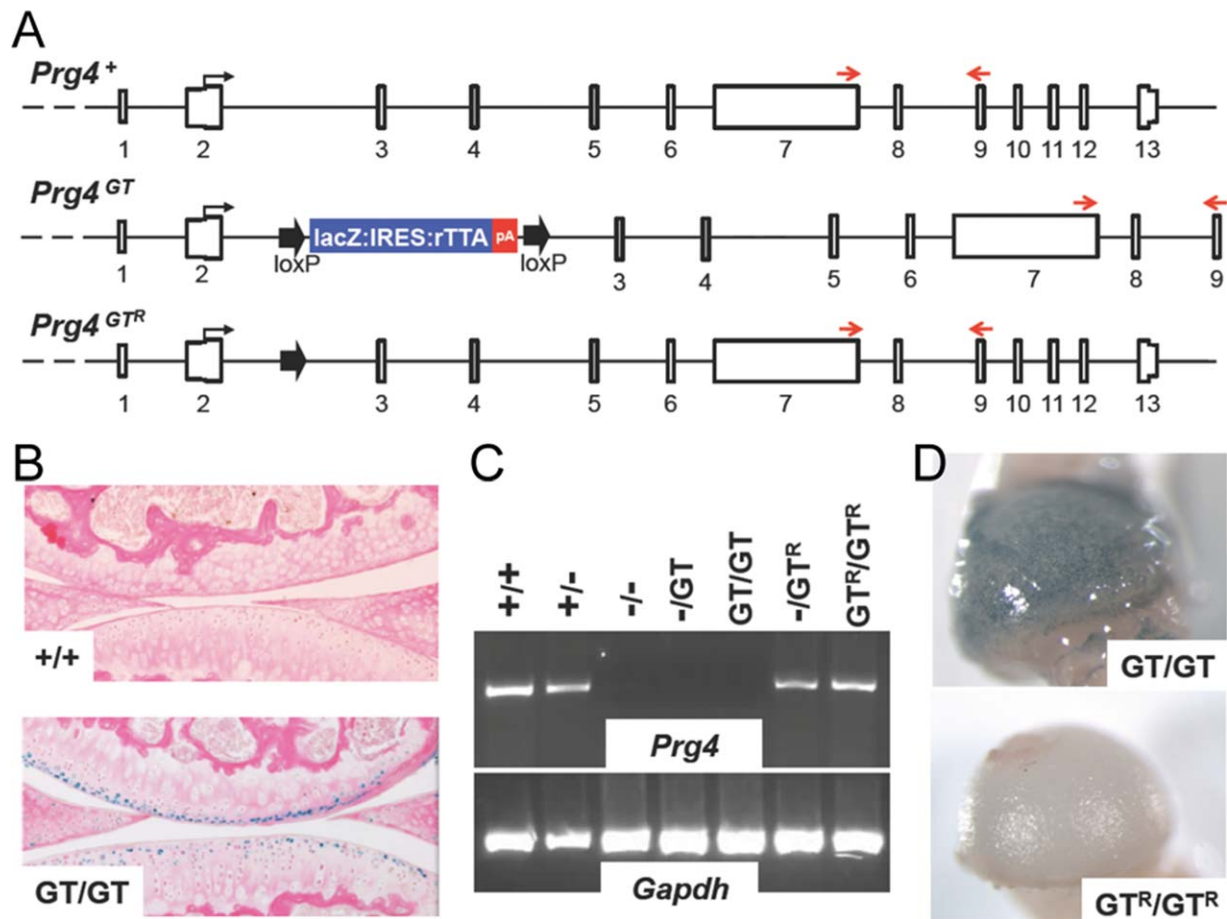


Figure 1. Generation of mice with a genetically engineered, Cre-excisable gene-trap (GT) in the second intron of *Prg4*. **A**, Schematic diagram depicting the genomic structure of the *Prg4* wild-type (+), GT, and Cre-recombined GT (GT^R) alleles. The GT is flanked by loxP sites (thick black arrows), which enable removal of the GT with Cre-recombinase. **B**, X-Gal staining for β -galactosidase activity in sagittal sections of the tibiofemoral joints of 2-month-old *Prg4* wild-type and homozygous GT mice. **C**, Semiquantitative reverse transcription–polymerase chain reaction (PCR) assessing *Prg4* mRNA transcript expression, relative to *Gapdh* as control, using total RNA extracted from the joints of mice with genotypes containing different combinations of *Prg4* wild-type, knockout (–), GT, and Cre-recombined GT alleles. The PCR primers are located downstream of the GT in *Prg4* exons 7 and 9 (as indicated by red arrows in **A**). **D**, Photomicrographs showing X-Gal staining for β -galactosidase activity in the femoral heads from 1-month-old mice homozygous for *Prg4* GT or Cre-recombined GT alleles. IRES = internal ribosome entry site; rtTA = reverse tetracycline *trans*-activator; pA = polyadenylation.

in PBS). Following staining, samples were washed in PBS, postfixed with PFA (4% w/v), and processed for histologic assessment in the same manner as described above.

Knee and femoral head cartilage samples were frozen in liquid nitrogen and homogenized in TRIzol (Invitrogen, Life Technologies) to recover RNA. For reverse transcription–polymerase chain reaction (RT-PCR) assays, RNA was isolated using a PureLink RNA Mini kit (Ambion) according to the manufacturer's instructions. Genomic DNA was removed by DNase I treatment. TaqMan RT reagents (Applied Biosystems, Life Technologies) were used to generate complementary DNA with oligo(dT). Semiquantitative PCR was performed using forward and reverse primers located within exons 7 and 9, respectively, since this region of *Prg4* is downstream of the gene-trap and not subject to alternative splicing in wild-type mice. *Gapdh* served as an internal control.

PCR products were separated on a 4% agarose gel and visualized using Sybr Safe (Invitrogen). RNA sequencing and data interpretation were performed as previously described (12,13).

Samples for biomechanical testing were harvested and soft tissue was removed around the tibiofemoral patellar joint, leaving the joint capsule intact. The whole-joint coefficient of friction (COF) was measured using a modified Stanton pendulum system, as previously described (7,14,15). During pendulum oscillation, motion was tracked with a Qalysis OPUS camera and Track Manager software (Qualysis) at a rate of 60 Hz. Oscillation data were processed with Visual3D software (C-Motion), and a custom MatLab code (MathWorks) was used to determine the peak amplitude of each cycle of oscillation and calculate the COF using a Stanton linear decay model (14).

Ex vivo cyclic loading was performed for 60 minutes, with the joint submerged in Dulbecco's modified Eagle's medi-

um (Life Technologies) to prevent desiccation. Loading was achieved using an active pendulum that was continuously oscillated at an angle of $\pm 15^\circ$ and at a rate of 1.5 Hz, in 15-minute increments (7). The whole-joint COF was measured at the end of each increment at room temperature in air. At the end of the loading experiment, each specimen was fixed in 10% formalin. Prior to immunostaining for activated caspase 3, each tissue specimen was decalcified at 4°C using a solution of 0.48M EDTA, adjusted to a pH of 7.1. Decalcified specimens were paraffin embedded.

Quantitative histologic assessment of the joint cartilage.

A tibiofemoral joint disease severity scoring system was devised based on several published scoring systems, including a scoring system from the Osteoarthritis Research Society International histopathology initiative (16–18), and included evaluation of surface damage, cartilage surface layer morphology, synovial hyperplasia, chondrocyte proliferation, and meniscus architecture. An additional score for meniscus integrity was included. The scoring system is summarized in Supplementary Table 1 (available on the *Arthritis & Rheumatology* web site at <http://onlinelibrary.wiley.com/doi/10.1002/art.39276/abstract>). Photomicrographs of the sagittal knee sections obtained from mice with different *Prg4* genotypes across several age groups were used to develop a training and reference set of images encompassing normal and diseased joints. Briefly, the knee sections were assessed for changes to surface morphologic features, synovial hyperplasia, chondrocyte proliferation, and meniscal architecture. The tibial plateau and the femoral condyle were scored separately. All samples were scored from H&E-stained sections. Three scientists (KAW, JMA, and GDJ), each of whom had received training on the scoring system, were sent 2 photomicrographs for each experimental animal. The scientists were blinded with respect to the animals' genotypes and treatment groups.

Activated caspase 3 immunostaining. Paraffin-embedded coronal sections (5 μm) were heated to 60°C for 30 minutes, deparaffinized, and hydrated in 3 changes of xylene alternating with alcohol. Sections were quenched in endogenous peroxidase in 3% hydrogen peroxide for 10 minutes, and antigen retrieval was performed using a pepsin solution (Thermo Scientific) following the manufacturer's recommendations. A rabbit polyclonal antibody against active caspase 3 (ab13847; Abcam), at a 1:50 dilution in staining buffer containing 8% (volume/volume) horse serum, was added to the sections and incubated at 4°C overnight. After 3 washes with PBS, the sections were incubated with Cy3-conjugated goat anti-rabbit IgG (Molecular Probes, Life Technologies), at a 1:50 dilution in staining buffer containing 8% (v/v) horse serum, for 1 hour at room temperature, protected from light. The sections were washed 5 times with PBS and counterstained using Vectashield mounting medium with DAPI (1.5 $\mu\text{g}/\text{ml}$; Vector Laboratories).

Images were captured with a 10 \times objective, using a Roper Scientific Photometrics CoolSNAP HQ2 monochrome camera connected to a Nikon Eclipse 90i microscope. Fluorescent images were set at a uniform threshold to reduce background autofluorescence and to adjust the DAPI signal, using Adobe Systems Photoshop CS5 software. Cells positive for activated caspase 3 were visualized at 100 \times magnification, using Image-Pro Plus 7.0 software. Activated caspase 3-positive chondrocytes and DAPI-stained nuclei from the entire thickness of the mouse cartilage on the medial and lateral tibial plateaus and femoral condyles were manually counted by a blinded observer (KAW), using corresponding H&E-stained

sections as a reference for cartilage depth. The overall percentage of activated caspase 3-positive chondrocytes among the total number of chondrocytes was reported.

Droplet digital PCR (ddPCR) assay of Cre-mediated recombination following tamoxifen administration in a 4-month-old mouse with the *ROSA26*^{CreERT2} allele. Tamoxifen was administered for 8 consecutive days to a 4-month-old mouse that was double homozygous for conditional *Pik3ca*^{H1047R} alleles (19) and *ROSA26*^{CreERT2} alleles. The mouse was killed 2 days after tamoxifen administration, and DNA was extracted from multiple tissue samples, including tissue from the tail, cerebral cortex, and femoral head articular cartilage. A ddPCR assay (20) was used to quantify the fraction of cells in the different tissue samples that had undergone Cre-mediated recombination.

A PCR primer pair (CAAGGGAGAGGAATGG-TAAGG and CAACTCAGGCATGCCGGATCCCAA) was used to generate a 719-bp amplicon from the conditional allele and a 265-bp amplicon from the recombined alleles. In addition, the PCR mixture contained fluorescent probes that detect the recombined allele (FAM-CGAAGTTATGT-TAACTTGTAGACC-IABk) or the conditional allele (HEX-CGAAGTTATTTGTTAGACCCTT-IABk). Seven nanograms of each DNA sample was tested in duplicate in 20- μl reaction mixtures that were emulsified into $\sim 14,000$ droplets using a QX100 Droplet Generator (Bio-Rad), according to the manufacturer's instructions. PCR was performed with the following parameters: 10 minutes at 95°C, followed by 40 cycles of 30 seconds at 94°C, 60 seconds at 55°C, and 120 seconds at 72°C, and then kept at 12°C. Samples were read using a QX100 Droplet Reader, and results were analyzed with QuantaSoft software (both from Bio-Rad).

Statistical analysis. Statistical analyses of whole-joint COFs, with comparisons between genotypes and between cyclic loading durations, were performed using two-way repeated-measures analysis of variance (ANOVA) ($\alpha = 0.05$) with Tukey's multiple comparison test, using GraphPad Prism statistical software (version 6). For statistical analyses of total joint histologic scores, the mean values of the 3 scientists' scores for each mouse were used. Total joint histologic scores were compared between genotypes, treatment groups, and time points, using the Mann-Whitney U test for nonparametric data, given the lack of normality of the data and because these values represent scores rather than continuous data. Interobserver agreement in histologic scores was measured with the intraclass correlation coefficient (ICC) with 95% confidence interval (95% CI). Statistical analyses were performed using IBM SPSS statistical software (version 21.0). Two-tailed *P* values less than 0.05 were considered significant. Comparisons of the percentage of activated caspase 3-positive cells between different genotypes were analyzed using one-way ANOVA ($\alpha = 0.05$) with Tukey's multiple comparison test, using GraphPad Prism statistical software (version 6). Due to their functional equivalence, the *Prg4*^{GT/GT}, *Prg4*^{GT/-}, and *Prg4*^{-/-} genotypes were combined into a single group for the purposes of statistical analyses, as were the *Prg4*^{+/-}, *Prg4*^{GT+/-}, *Prg4*^{+GT}, and *Prg4*^{GT^R/GT} genotypes.

RESULTS

Generation of mice with a reversible gene-trap in *Prg4*. Mice with the gene-trap allele (Figure 1A) were generated and bred to either a homozygous

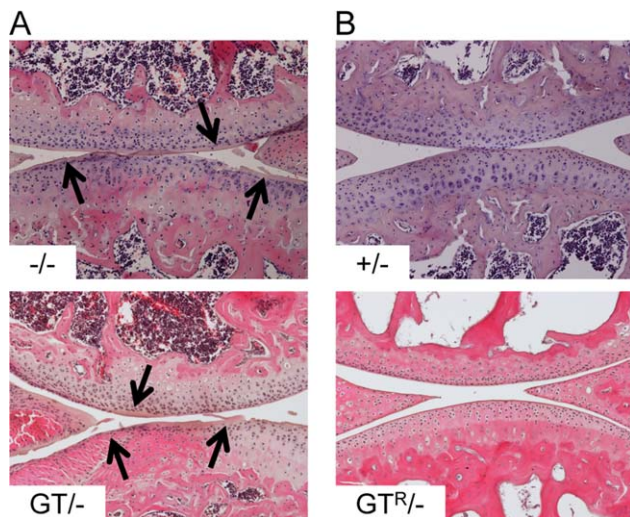


Figure 2. The *Prg4* gene-trap (GT) allele is a loss-of-function allele whose function is fully restored following Cre-mediated excision. **A**, Hematoxylin and eosin (H&E) staining of the tibiofemoral joints from 2-month-old *Prg4* homozygous knockout (-/-) and compound heterozygous GT/knockout (GT⁻) mice. **Arrows** indicate protein deposition along the cartilage surface, consistent with lubricin deficiency. **B**, H&E staining of the tibiofemoral joints from 2-month-old *Prg4* heterozygous knockout (+/-) and compound heterozygous Cre-recombined GT/knockout (GT^R/-) mice. The articular cartilage in these mice appears to be normal, in that the superficial zone chondrocyte nuclei are located adjacent to the cartilage surface, the internal edges of the menisci are sharp, and there is no protein deposition along the surface. Original magnification $\times 100$.

(*Prg4*^{GT/GT}) or compound heterozygous (*Prg4*^{GT/-} and *Prg4*^{GT/+}) genotype. The gene-trap allele was found to produce β -galactosidase instead of lubricin, as indicated by X-Gal staining of *Prg4*^{GT/GT} mouse cartilage (Figure 1B). Furthermore, *Prg4*^{GT/GT} mice did not express wild-type *Prg4* messenger RNA (mRNA), as indicated by RT-PCR using *Prg4* primers in exons that are downstream of the gene-trap (Figure 1C) and as shown by RNA sequencing (details in Supplementary Figure 1A, available on the *Arthritis & Rheumatology* web site at <http://onlinelibrary.wiley.com/doi/10.1002/art.39276/abstract>).

To determine whether Cre-mediated excision of the gene-trap restored endogenous *Prg4* mRNA expression, we excised the gene-trap in germ cells using the Tg(*ell* α -Cre) allele to generate mice with a *Prg4*^{GT^R} allele (Figure 1A), and bred the *Prg4*^{GT^R} allele to either a homozygous (*Prg4*^{GT^R/GT^R}) or compound heterozygous (*Prg4*^{GT^R/-}) genotype. Unlike *Prg4*^{GT/GT} mouse articular chondrocytes, *Prg4*^{GT^R/GT^R} mouse articular chondrocytes expressed lubricin mRNA (Figure 1C) and no longer expressed β -galactosidase (Figure 1D). We performed RNA sequencing on the knee joint cartilage from 2- and 3-week-old *Prg4*^{+/+}, *Prg4*^{GT/GT}, *Prg4*^{GT^R/-}, *Prg4*^{+/+},

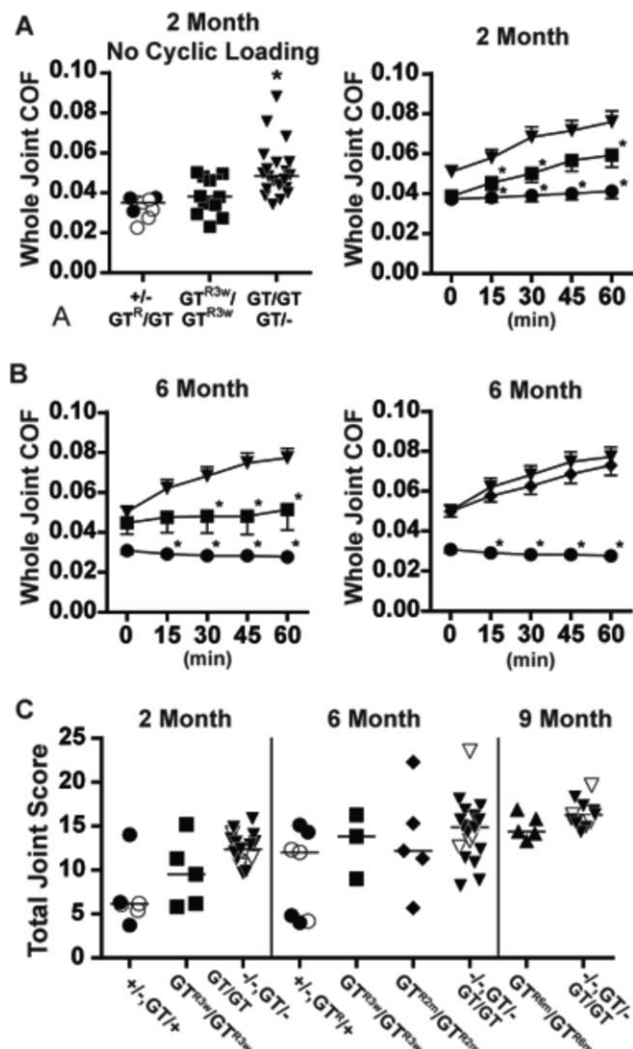


Figure 3. Tibiofemoral patellar whole-joint coefficients of friction (COFs) (A and B) and total joint histologic disease severity scores (C) are affected by animal age and *Prg4* genotype. **A**, Left, Individual COFs in the joints of 2-month-old lubricin-sufficient mice (*Prg4* heterozygous knockout [+/-] [○] and Cre-recombined gene-trap [GT^R]/GT [●]), lubricin-deficient mice (GT/GT and GT/- [▼]), and mice with lubricin reexpressed at age 3 weeks (GT^{R3w}/GT^{R3w}) (■). Horizontal bars indicate the median. Right, Mean COFs during ex vivo cyclic loading of the joints of lubricin-sufficient mice (n = 3) (●), lubricin-deficient mice (n = 20) (▼), and GT^{R3w}/GT^{R3w} mice (n = 12) (■). **B**, Left, Mean COFs during cyclic loading of the joints of 6-month-old lubricin-sufficient mice (GT^R/-) (n = 3) (●), lubricin-deficient mice (GT/- and GT/GT) (n = 14) (▼), and GT^{R3w}/GT^{R3w} mice (n = 7) (■). Right, Same COF measurements as on the left, except using mice in which lubricin was reexpressed at age 2 months (GT^{R2m}/GT^{R2m}) (n = 14) (◆). Values in A (right) and B are the mean \pm SEM. * = *P* < 0.05 versus the other groups. **C**, Individual total joint histologic scores at ages 2 months, 6 months, or 9 months in lubricin-sufficient mice (+/- [○] or GT/+ [●]), lubricin-deficient mice (-/- [▽] or GT/- [▼]) and GT/GT [▼]), GT^{R3w}/GT^{R3w} mice (■), GT^{R2m}/GT^{R2m} mice (◆), and mice with lubricin reexpressed at age 6 months (GT^{R6m}/GT^{R6m}) (▲). Horizontal bars indicate the mean. Cohort sizes and *P* values for between-group comparisons are reported in Table 1.

Prg4^{GT^R/GT}, and *Prg4*^{+ /GT} mice, and confirmed that the GT allele is a null allele (see Supplementary Figures 1A and B, available on the *Arthritis & Rheumatology* web site at <http://onlinelibrary.wiley.com/doi/10.1002/art.39276/abstract>). We also confirmed that the abundance of the GT^R allele (see Supplementary Figure 1B) and the splice forms from the GT^R allele (data not shown) are the same as those from the wild-type allele.

Identification of the *Prg4*^{GT} allele as a loss-of-function allele, and the *Prg4*^{GT^R} allele as an apparent wild-type allele. Histologic assessment of the tibiofemoral cartilage of 2-month-old *Prg4*^{-/-} and *Prg4*^{GT/-} mice revealed similar histopathologic changes to the cartilage in both genotypes (Figure 2A), consistent with the notion that the *Prg4*^{GT} allele prevents lubricin expression. Conversely, the histologic appearance of the cartilage of *Prg4*^{+/-} and *Prg4*^{GT^R/-} mice was normal (Figure 2B), both being indistinguishable from that of wild-type mouse cartilage, indicating that *Prg4*^{GT^R} functions in a manner similar to a wild-type allele. Moreover, in mice at age 2 months, protein deposition was apparent on the cartilage surface in both the *Prg4*^{-/-} and *Prg4*^{GT/-} genotypes, but was not apparent in either the *Prg4*^{+/-} or *Prg4*^{GT^R/-} genotype (Figures 2A and B).

Consistent with the abnormal appearance of the articular cartilage of lubricin-deficient mice, these mice (i.e., mice with the *Prg4*^{GT/GT} or *Prg4*^{GT/-} genotype) had higher whole-joint COFs compared to lubricin-sufficient mice (i.e., mice with the *Prg4*^{+/-} or *Prg4*^{GT^R/GT} genotype) (Figure 3A and Table 1). In addition, the joints of lubricin-deficient mice exhibited a progressive increase in the COF during ex vivo cyclic loading, whereas the joints of lubricin-sufficient mice showed no notable changes in the COF during ex vivo cyclic loading (Figures 3A and B).

The total joint histologic scores assessed in the knees of 150 mice with different *Prg4* genotypes and ages (data not shown) were used to determine the ICC among the 3 scorers. The ICC was 0.922 (95% CI 0.897–0.941), indicating high correlation of scores. As expected, the total joint histologic scores were significantly better in 2-month-old lubricin-sufficient mice (i.e., *Prg4*^{+/-} and *Prg4*^{GT/+} mice) than in lubricin-deficient mice (i.e., *Prg4*^{GT/GT}, *Prg4*^{-/-}, and *Prg4*^{GT/-} mice) (Figure 3C and Table 1). Moreover, the total joint histologic scores of lubricin-deficient mice significantly worsened from ages 2 months to 6 months and from ages 6 months to 9 months (Figure 3C and Table 1). In contrast, no worsening in the total joint histologic score was observed in lubricin-sufficient mice when they were examined from ages 2 months to 6 months ($P = 0.628$), although there was greater variability in the total joint

Table 1. Differences in whole-joint coefficients of friction, total joint histologic scores, and percentages of activated caspase 3–positive chondrocytes in mice by age group and genotype*

Articular cartilage measure, age, genotype	<i>P</i>
Coefficient of friction	
2 mo LS (n = 9) vs. 6 mo LS (n = 3)	0.792
2 mo LD (n = 20) vs. 6 mo LD (n = 14)	0.863
2 mo LS (n = 9) vs. 2 mo LD (n = 20)	<0.001
2 mo LS (n = 9) vs. 2 mo GT ^{R3w} (n = 12)	0.217
2 mo GT ^{R3w} (n = 12) vs. 2 mo LD (n = 20)	0.003
6 mo LS (n = 3) vs. 6 mo LD (n = 14)	0.006
6 mo LS (n = 3) vs. 6 mo GT ^{R3w} (n = 7)	0.069
6 mo GT ^{R3w} (n = 7) vs. 6 mo LD (n = 14)	0.270
6 mo GT ^{R2m} (n = 5) vs. 6 mo LD (n = 14)	0.937
Total joint histologic score	
2 mo LS (n = 6) vs. 6 mo LS (n = 7)	0.628
2 mo LD (n = 7) vs. 6 mo LD (n = 20)	0.020
6 mo LD (n = 20) vs. 9 mo LD (n = 11)	0.032
2 mo LS (n = 6) vs. 2 mo LD (n = 17)	0.006
2 mo LS (n = 6) vs. 2 mo GT ^{R3w} (n = 6)	0.180
2 mo GT ^{R3w} (n = 6) vs. 2 mo LD (n = 17)	0.062
6 mo LS (n = 7) vs. 6 mo LD (n = 20)	0.026
6 mo GT ^{R3w} (n = 3) vs. 6 mo LD (n = 20)	0.698
6 mo GT ^{R2m} (n = 5) vs. 6 mo LD (n = 20)	0.488
9 mo GT ^{R6m} (n = 5) vs. 9 mo LD (n = 11)	0.145
Activated caspase 3	
2 mo LS (n = 3) vs. 2 mo LD (n = 19)	<0.001
2 mo GT ^{R3w} (n = 12) vs. 2 mo LD (n = 19)	<0.001
2 mo GT ^{R3w} (n = 12) vs. LS (n = 3)	0.96
6 mo LS (n = 3) vs. 6 mo LD (n = 13)	<0.001
6 mo GT ^{R3w} (n = 3) vs. 6 mo LD (n = 13)	<0.001
6 mo GT ^{R3w} (n = 6) vs. 6 mo LS (n = 3)	0.92
6 mo GT ^{R2m} (n = 12) vs. 6 mo LD (n = 13)	0.77
6 mo GT ^{R2m} (n = 12) vs. 6 mo LS (n = 3)	0.001
6 mo GT ^{R3w} (n = 6) vs. 6 mo GT ^{R2m} (n = 12)	<0.001

* Comparisons were made between 2-, 6-, and 9-month-old (mo) mice with the following genotypes: lubricin-sufficient (LS) = +/+, GT^R/-, GT^R/GT, or +/GT; lubricin-deficient (LD) = -/-, GT/-, or GT/GT; GT^{R3w} = gene-trap reversed at age 3 weeks; GT^{R2m} = gene-trap reversed at age 2 months; and GT^{R6m} = gene-trap reversed at age 6 months. The coefficient of friction was measured without ex vivo cyclic loading (time = 0), and *P* values were determined by 2-tailed analysis of variance (ANOVA). *P* values for comparisons of the total joint histologic scores were determined by nonparametric Mann-Whitney U test. *P* values for comparisons of the percentage of activated caspase 3–positive chondrocytes were determined by one-way ANOVA. *P* values less than 0.05 were considered significant.

histologic scores of the 6-month-old lubricin-sufficient mice (Figure 3C and Table 1).

Partial histologic and biomechanical benefit of restoring lubricin expression in 3-week-old mice.

Having demonstrated that reversing the *Prg4*^{GT} allele (i.e., *Prg4*^{GT^R}) prior to conception prevented cartilage damage, we next determined whether restoring lubricin expression after birth would be beneficial. To induce Cre-mediated excision of the gene-trap after birth, we utilized the *ROSA26*^{CreER12} allele. We generated *Prg4*^{GT/+}, *Prg4*^{GT/GT}, and *Prg4*^{GT/GT};*ROSA26*^{CreER12/+} mice, and at age 3 weeks, the mice received 10 daily

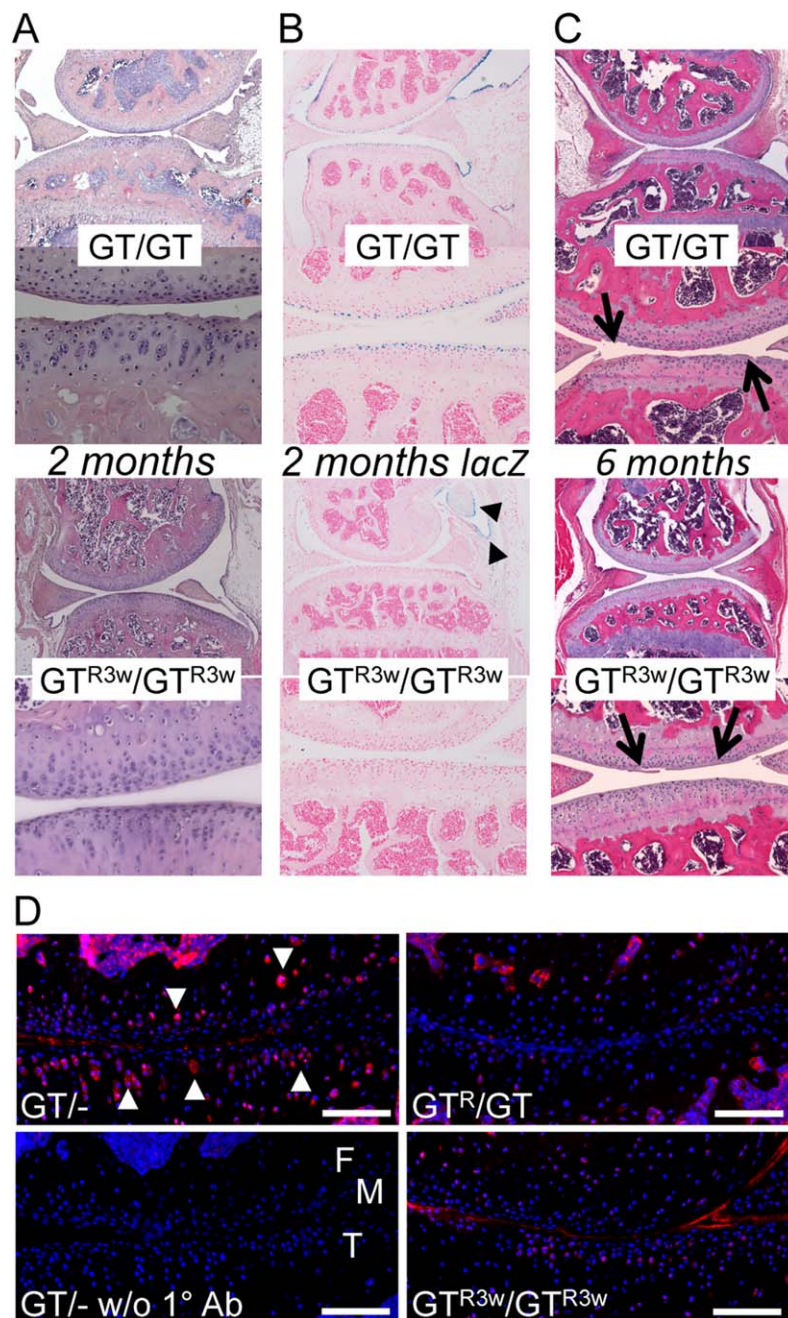


Figure 4. Restoring *Prg4* expression in 3-week-old mice may delay, but does not prevent, histopathologic appearance of cartilage damage. **A** and **B**, Hematoxylin and eosin (H&E) (**A**) and X-Gal (**B**) staining of cartilage sections from the tibiofemoral joints of 2-month-old mice homozygous for the gene-trap (GT) allele or homozygous for a GT allele that had been Cre-excised at age 3 weeks (GT^{R3w}/GT^{R3w}). **Arrowheads** indicate that some regions of the synovium still express LacZ, providing evidence that Cre-mediated recombination of the GT allele in synovium is incomplete. **C**, H&E staining of cartilage sections from the joints of 6-month-old GT/GT or GT^{R3w}/GT^{R3w} mice. **Arrows** indicate that protein deposition is present on the surface of the GT^{R3w}/GT^{R3w} mouse cartilage, although the morphology of the superficial zone chondrocytes is less severely affected as compared to that of GT/GT mouse cartilage. Original magnification $\times 40$ (top panels) and $\times 200$ (bottom panels). **D**, Immunostaining for activated caspase 3 following 60 minutes of ex vivo cyclic loading of the joints of 2-month-old lubricin-deficient mice (GT/-), lubricin-sufficient mice (GT^R/GT), and GT^{R3w}/GT^{R3w} mice. Cell nuclei are labeled with DAPI. Omission of primary antibody (w/o 1° Ab) in GT/- mouse cartilage results in no staining. The locations of the femoral condyle (F), meniscus (M), and tibia (T) are also shown. **Arrowheads** indicate examples of chondrocytes that are positive for activated caspase 3. Bars = 100 μ m. Cohort sizes and *P* values for between-group comparisons of the percentages of activated caspase 3-containing chondrocytes are reported in Table 1.

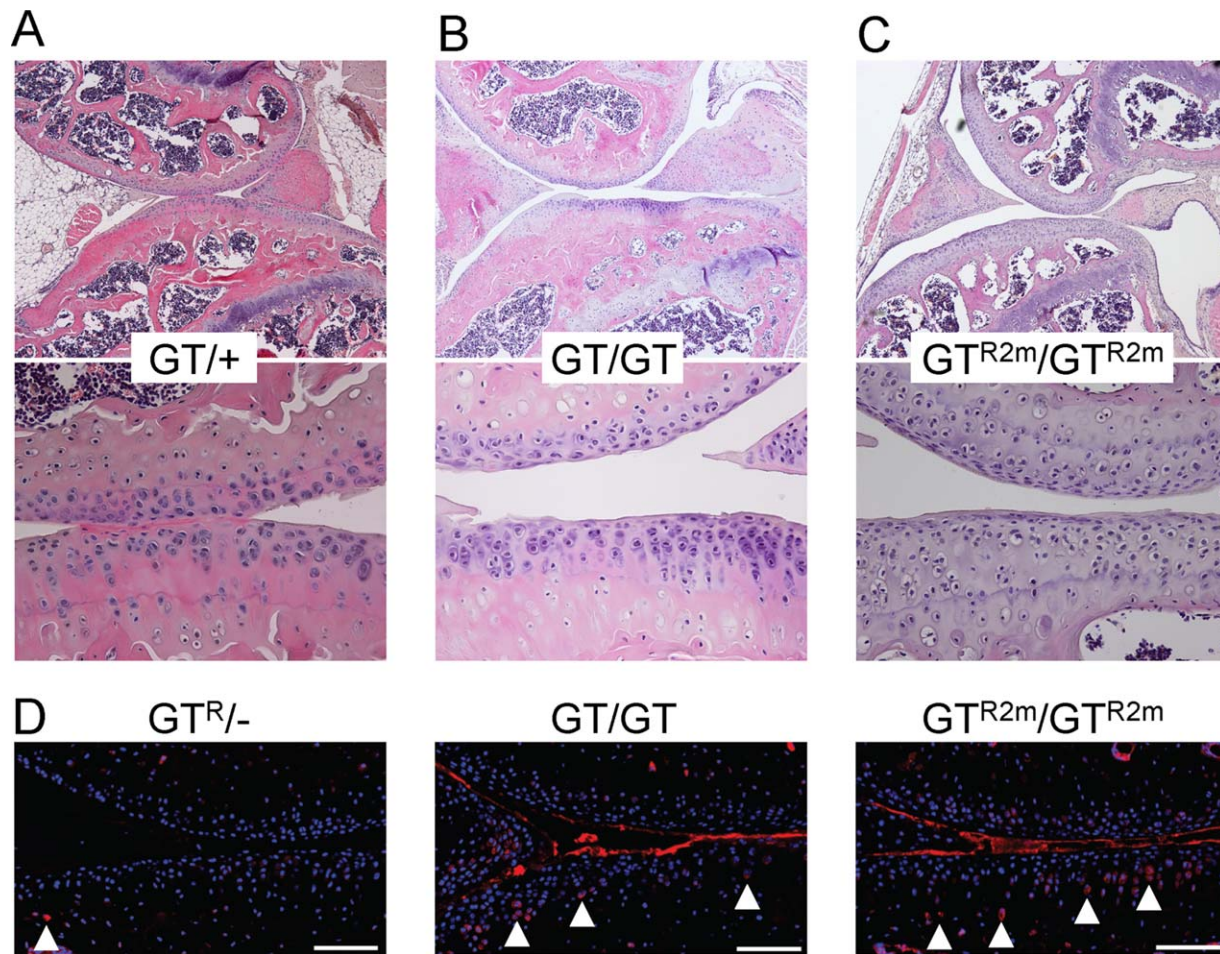


Figure 5. Restoring *Prg4* expression in mice at age 2 months does not improve the histologic appearance of the articular cartilage. **A–C**, Hematoxylin and eosin staining of cartilage sections from the tibiofemoral joints of a 6-month-old heterozygous gene-trap (GT) mouse (**A**), a homozygous GT mouse (**B**), and a mouse whose GT was Cre-excised at age 2 months (GT^{R2m}/GT^{R2m}) (**C**). Original magnification $\times 40$ (top panels) and $\times 200$ (bottom panels). **D**, Immunostaining for activated caspase 3 following 60 minutes of ex vivo cyclic loading of the joints of a 6-month-old lubricin-sufficient mouse ($GT^{R/-}$), a lubricin-deficient mouse (GT/GT), and a GT^{R2m}/GT^{R2m} mouse. Cell nuclei are labeled with DAPI. **Arrowheads** indicate examples of chondrocytes that are positive for activated caspase 3. Bars = 100 μm . Cohort sizes and *P* values for between-group comparisons of the percentages of activated caspase 3-containing chondrocytes are reported in Table 1.

intraperitoneal injections of tamoxifen or vehicle alone. Thereafter, when the mice reached ages 2 months and 6 months, we examined the knee joints biomechanically using whole-joint COFs (Figures 3A and B and Table 1), and histologically using total joint histologic scores and immunostaining (Figures 3C and 4A–D, and Table 1). We confirmed that 10 days of tamoxifen injections led to efficient excision of the gene-trap in the superficial zone chondrocytes of $Prg4^{GT/GT};ROSA26^{CreERT2/+}$ mice, as indicated by X-Gal staining of the cartilage sections from mice at age 2 months (Figure 4B).

After the $Prg4^{GT/GT};ROSA26^{CreERT2/+}$ mice had been treated with tamoxifen at age 3 weeks, the joints of these mice (i.e., $Prg4^{GT^{R3w}/GT^{R3w}}$ mice) had lower COFs at

age 2 months ($P < 0.003$) and trended toward having better-appearing cartilage based on histologic features and lower total joint histologic scores ($P = 0.062$) compared to lubricin-deficient mice (Figures 3A–C and Table 1). The histologic appearance nevertheless appeared worse than that of mice with an inherited functional allele (e.g., $Prg4^{+}$ and $Prg4^{GT^R}$) (Figures 2B, 3C, and 4), but this difference did not achieve statistical significance (Table 1).

Biomechanical testing showed that restoring lubricin expression in mice at age 3 weeks resulted in a significant reduction in the COF compared to that in littermates with nonfunctional alleles. Moreover, the COF increased in mice with restored lubricin expression at age 3 weeks as compared to mice with inherited func-

tional alleles, but the difference was not significant (Figures 3A and B). Interestingly, however, in contrast to that in mice with inherited functional alleles, ex vivo cyclic loading of the joints of $Prg4^{GT^{R3w}/GT^{R3w}}$ mice was associated with a progressive increase in the COF (Figure 3B).

We then determined the percentage of chondrocytes that were positive for activated caspase 3 following cyclic loading. We found that significantly fewer cells exhibited activated caspase 3 in $Prg4^{GT^{R3w}/GT^{R3w}}$ mice compared to lubricin-deficient littermates (Figure 4D and Table 1). In addition, we observed no difference in the percentage of activated caspase 3–positive chondrocytes between $Prg4^{GT^{R3w}/GT^{R3w}}$ and $Prg4^{GT^{R}/-}$ mice ($P = 0.96$).

In $Prg4^{GT^{R3w}/GT^{R3w}}$ mice at age 6 months, the joint COF became higher than that in mice with inherited functional alleles. When compared to lubricin-deficient mice, the COF in $Prg4^{GT^{R3w}/GT^{R3w}}$ mice at age 6 months was not significantly different (Figure 3B and Table 1). However, the joints of 6-month-old $Prg4^{GT^{R3w}/GT^{R3w}}$ mice did not show a progressive increase in the COF with cyclic loading, in contrast to that in their lubricin-deficient littermates (Figure 3B), and the percentage of activated caspase 3–positive chondrocytes in the cyclically loaded joints of 6-month-old $Prg4^{GT^{R3w}/GT^{R3w}}$ mice was lower than that in the cyclically loaded joints of lubricin-deficient mice (Table 1). However, we could no longer detect a quantifiable improvement in the histopathologic features of the articular cartilage of 6-month-old $Prg4^{GT^{R3w}/GT^{R3w}}$ mice as compared to lubricin-deficient mice (Figures 3C and 4C, and Table 1).

Lack of histologic or biomechanical benefit from restoring $Prg4$ expression in 2-month-old mice. Having found partial benefit from restoring gene expression in 3-week-old mice, we next restored gene expression in 2-month-old mice (i.e., $Prg4^{GT^{R2m}/GT^{R2m}}$ mice). When the mice reached age 6 months, we examined their joints histologically and biomechanically. Cartilage histologic features, the whole-joint COF, and the percentage of cells positive for activated caspase 3 were no better in $Prg4^{GT^{R2m}/GT^{R2m}}$ mice than in lubricin-deficient mice (Figures 3 and 5, and Table 1), with most of the activated caspase 3–positive cells located in the middle, rather than superficial, articular cartilage zone. Similarly, we observed no histologic benefit of restoring lubricin expression in the joints of these mice at age 6 months when examined at age 9 months (Figure 3C and Table 1).

Similar to the findings reported by other investigators (21), we confirmed that the $ROSA26^{CreERT2}$ allele remained active in older mice, as indicated by RNA sequencing of the cartilage tissue from $Prg4^{GT^{R6m}/GT^{R6m}}$

mice immediately after they had received tamoxifen for 10 consecutive days (see Supplementary Figure 1B, available on the *Arthritis & Rheumatology* web site at <http://onlinelibrary.wiley.com/doi/10.1002/art.39276/abstract>) and as demonstrated by the results of the ddPCR assay. In our experiments assessing a 4-month-old mouse that was double homozygous for the $Pik3ca^{H1047R}$ and $ROSA26^{CreERT2}$ alleles, we found that >98% of articular cartilage chondrocytes underwent Cre-mediated recombination immediately after the mouse had received tamoxifen for 8 consecutive days (see Supplementary Figure 1C).

DISCUSSION

Degenerative joint disease is common (22,23). In the context of a severe joint injury, the initiating event is known (24,25). However, in most patients with osteoarthritis, the incipient event, if one exists, is not known. We used a genetic mouse model of progressive joint failure (i.e., lubricin-deficient mice), caused by inadequate boundary lubrication at the cartilage surface, to determine whether cartilage damage can be ameliorated by restoring the boundary lubricant and, if so, whether there is a window of opportunity for successfully intervening. These questions are of primary importance for the management of patients with CACP, who have congenital lubricin deficiency, and may be important for individuals with acquired deficiency of lubricin, as can occur during injury, infection, and inflammatory disease (26).

We restored lubricin expression in lubricin-deficient mice using a Cre-excisable $Prg4$ gene-trap (Figure 1). We first showed that removal of the gene-trap recreates a wild-type allele (Figure 2). We then evaluated mice in which we removed the gene-trap at age 3 weeks, and observed an improved, but not normal, histologic appearance of their tibiofemoral cartilage at age 2 months (Figures 3 and 4). The whole-joint COF in these mice was also improved, but not normalized, at age 2 months (Figure 3); however, we could no longer detect an overall improvement in the histologic appearance or in the COF of the articular cartilage of 6-month-old mice (Figures 3 and 4). The histologic appearance of the joints, or at least the total joint histologic scoring system that we used, may not accurately reflect joint function in these mice, since even lubricin-sufficient mice developed higher and more variable joint disease severity scores as they aged. Biomechanical function during cyclic loading along with measurement of activated caspase 3 may provide a more sensitive method for assessing the effect, or lack thereof, of lubricin restoration (Figures 3 and 4). Based on biomechanical testing and activated caspase 3 staining, restoring

lubricin expression in 3-week-old mice produced some beneficial effect.

Restoring lubricin expression in 2-month-old mice produced no apparent benefit (Figures 3 and 5). These data imply that the therapeutic window of opportunity for preventing irreversible cartilage damage in congenital lubricin deficiency is small, at least in this animal model. The relationship of therapeutic windows between mice and humans is unknown. However, it seems likely that early intervention will be required in order to prevent or delay cartilage failure in patients with CACP.

Recent findings indicate that lubricin may promote cell preservation by providing anabolic signaling (27) and preventing apoptosis. A significant reduction in the percentage of activated caspase 3–positive cells in mice subjected to Cre-mediated recombination at age 3 weeks, as compared to that in lubricin-deficient mice, indicates that cellular protection is reestablished following recombination. As the sole cell type in cartilage, chondrocytes play specialized roles in the maintenance of the cartilage extracellular matrix. The majority of activated caspase 3–positive chondrocytes were rounded and were found in the upper middle zone, located just below the flattened superficial chondrocytes. Based on previous findings in bovine cartilage (28–30) and studies regarding the structure of collagen in mouse cartilage (31), we hypothesize that the junction of tangential to columnar type II collagen bundles in this region results in elevated cartilage strain that damages rounded chondrocytes, which are not designed to withstand shear stress. Furthermore, elevated stress may contribute to a number of transduction pathways, including the expression of catabolic and apoptotic factors (32–39), which accelerate cartilage deterioration in the disease state.

Our results may be relevant to common forms of degenerative joint disease. Excessive friction has been shown to cause apoptosis in bovine cartilage bearings (15,40). We observed excessive caspase 3 activation following cyclic loading in lubricin-deficient mice (Figures 4 and 5, and Table 1) and in gene-trap mice whose lubricin expression was restored at age 2 months (Figure 5). Thus, patients with a transient deficiency of boundary lubrication may sustain cartilage damage that will progress, even after the lubricin levels have returned to normal.

If transiently increased friction within a joint is an incipient event for degenerative joint disease, then strategies for preventing or rapidly reducing friction are needed. Five published studies have demonstrated beneficial effects of administering lubricin following joint injury in animal models (41–45). However, each of these

studies had limited followup—between 28 days and 70 days following joint injury—and, therefore, it remains uncertain whether adding lubricin would really prevent, or might only delay, joint failure. Interestingly, constitutive overexpression of lubricin has been demonstrated to prevent cartilage damage in a mouse model of traumatic joint injury, although the length of followup was <6 weeks (27).

The strength of our study is in its genetic approach. By placing the gene-trap into the *Prg4* locus, we were able to restore endogenous lubricin mRNA expression when the gene-trap was excised. Moreover, since lubricin mRNA has several different splice forms, our genetic approach restored expression of all forms. However, we could not demonstrate that lubricin protein was produced when the gene-trap was excised, since we have not been able to generate antibodies (46) or find a commercially available antibody that reliably immunodetects mouse lubricin when *Prg4*^{-/-} mice are used as an appropriate negative control. Instead, we inferred that protein was being expressed on the basis of the observed normal phenotypes of *Prg4*^{GT^R/GT^R} and *Prg4*^{GT^R/-} mice, the reappearance of *Prg4* mRNA demonstrated by RT-PCR (Figure 1) and RNA sequencing in mice with the *Prg4*^{GT^R} allele (see Supplementary Figure 1, available on the *Arthritis & Rheumatology* web site at <http://onlinelibrary.wiley.com/doi/10.1002/art.39276/abstract>), and the loss of β -galactosidase expression in chondrocytes and most synoviocytes from which the *Prg4*^{GT} allele had been Cre-excised (Figure 4).

There are several limitations to our study. First, some cohorts were underpowered to achieve statistical significance. Faster and more reliable imaging techniques are being developed to assess cartilage morphology, which should make studies involving larger sized cohorts more feasible.

Second, scattered areas of β -galactosidase expression were still present in the synovium of treated mice, indicating that we had not restored lubricin expression in every type B synoviocyte. Therefore, we may not have attained normal lubricin levels in the synovial fluid.

Third, the genetic background of the mice used in this study was mostly C57BL/6J, a background in which full-thickness cartilage defects are known to heal less well than in other strains of mice (47). Therefore, mice with other genetic backgrounds might have had better responses to lubricin reexpression.

Finally, despite having an ICC of >0.9, the histologic scoring system used in the present study may be insensitive with regard to detection of chondroprotective effects. In a study of preclinical rodent OA lubricin supplementation, a modified Mankin histologic scoring

system failed to show improvement of cartilage damage, but levels of urine type II collagen degradation products were significantly lower in the rodents treated with exogenous lubricin (42). Longer-term followup and more sensitive measures of joint structure and function may be needed to better assess therapeutic outcomes.

Future work is also needed to determine whether restoration of lubricin expression in mice younger than age 3 weeks can reverse disease or prevent disease progression. It is possible that lubricin assumes a critical function during joint cavitation that is irreplaceable after birth, although the cartilage of newborn lubricin-deficient mice appeared normal by electron microscopy (6). In addition, the present studies were performed in mice that had congenital deficiency of lubricin, as is also seen in patients with CACP. Studies in mice in which the joints had formed when lubricin was sufficient and which then developed a transient deficiency would better inform us regarding the importance of preventing transient deficiency in traumatic injuries and inflammatory disorders.

Thus, our data suggest that early restoration of lubricin expression may slow disease progression in patients with CACP, a condition in which individuals congenitally lack this protein. Further studies are required to determine the relevance of our findings in the management of patients experiencing transient acquired deficiency of lubricin due to traumatic injury or inflammation.

ACKNOWLEDGMENT

We thank Dr. Minjie Zhang for helping process the cartilage samples for the ddPCR and RNA sequencing analyses.

AUTHOR CONTRIBUTIONS

All authors were involved in drafting the article or revising it critically for important intellectual content, and all authors approved the final version to be published. Drs. Warman and Jay had full access to all of the data in the study and take responsibility for the integrity of the data and the accuracy of the data analysis.

Study conception and design. Hill, Waller, Cui, Hann, Zurakowski, Warman, Jay.

Acquisition of data. Hill, Waller, Cui, Smits, Zhang, Ayturk, Hann, Lessard, Jay.

Analysis and interpretation of data. Hill, Waller, Cui, Allen, Smits, Zhang, Ayturk, Hann, Lessard, Zurakowski, Warman, Jay.

REFERENCES

- Von Porat A, Roos EM, Roos H. High prevalence of osteoarthritis 14 years after an anterior cruciate ligament tear in male soccer players: a study of radiographic and patient relevant outcomes. *Ann Rheum Dis* 2004;63:269–73.
- Marcelino J, Carpten JD, Suwairi WM, Gutierrez OM, Schwartz S, Robbins C, et al. CACP, encoding a secreted proteoglycan, is mutated in camptodactyly-arthropathy-coxa vara-pericarditis syndrome. *Nat Genet* 1999;23:319–22.
- Jay GD, Britt DE, Cha CJ. Lubricin is a product of megakaryocyte stimulating factor gene expression by human synovial fibroblasts. *J Rheumatol* 2000;27:594–600.
- Rhee DK, Marcelino J, Baker M, Gong Y, Smits P, Lefebvre V, et al. The secreted glycoprotein lubricin protects cartilage surfaces and inhibits synovial cell overgrowth. *J Clin Invest* 2005;115:622–31.
- Schumacher BL, Hughes CE, Kuettner KE, Caterson B, Aydelotte MB. Immunodetection and partial cDNA sequence of the proteoglycan, superficial zone protein, synthesized by cells lining synovial joints. *J Orthop Res* 1999;17:110–20.
- Jay GD, Torres JR, Rhee DK, Helminen HJ, Hytinen MM, Cha CJ, et al. Association between friction and wear in diarthrodial joints lacking lubricin. *Arthritis Rheum* 2007;56:3662–9.
- Drewniak EI, Jay GD, Fleming BC, Zhang L, Warman ML, Crisco JJ. Cyclic loading increases friction and changes cartilage surface integrity in lubricin-mutant mouse knees. *Arthritis Rheum* 2012;64:465–73.
- Albuhairan I, Al-Mayouf SM. Camptodactyly-arthropathy-coxavara-pericarditis syndrome in Saudi Arabia: clinical and molecular genetic findings in 22 patients. *Semin Arthritis Rheum* 2013;43:292–6.
- Anderson DD, Chubinskaya S, Guilak F, Martin JA, Oegema TR, Olson SA, et al. Post-traumatic osteoarthritis: improved understanding and opportunities for early intervention. *J Orthop Res* 2011;29:802–9.
- Friedel RH, Plump A, Lu X, Spilker K, Jolicoeur C, Wong K, et al. Gene targeting using a promoterless gene trap vector (“targeted trapping”) is an efficient method to mutate a large fraction of genes. *Proc Natl Acad Sci U S A* 2005;102:13188–93.
- Schmitz N, Laverty S, Kraus VB, Aigner T. Basic methods in histopathology of joint tissues. *Osteoarthritis Cartilage* 2010;18 Suppl 3:S113–6.
- Ayturk UM, Jacobsen CM, Christodoulou DC, Gorham J, Seidman JG, Seidman CE, et al. An RNA-seq protocol to identify mRNA expression changes in mouse diaphyseal bone: applications in mice with bone property altering *Lrp5* mutations. *J Bone Miner Res* 2013;28:2081–93.
- Kozhemyakina E, Zhang M, Ionescu A, Ayturk UM, Ono N, Kobayashi A, et al. Identification of a *Prg4*-expressing articular cartilage progenitor cell population in mice. *Arthritis Rheumatol* 2015;67:1261–73.
- Drewniak EI, Jay GD, Fleming BC, Crisco JJ. Comparison of two methods for calculating the frictional properties of articular cartilage using a simple pendulum and intact mouse knee joints. *J Biomech* 2009;42:1996–9.
- Waller KA, Zhang LX, Elsaid KA, Fleming BC, Warman ML, Jay GD. Role of lubricin and boundary lubrication in the prevention of chondrocyte apoptosis. *Proc Natl Acad Sci U S A* 2013;110:5852–7.
- Glasson SS, Chambers MG, Van Den Berg WB, Little CB. The OARSI histopathology initiative: recommendations for histological assessments of osteoarthritis in the mouse. *Osteoarthritis Cartilage* 2010;18 Suppl 3:S17–23.
- Coles JM, Zhang L, Blum JJ, Warman ML, Jay GD, Guilak F, et al. Loss of cartilage structure, stiffness, and frictional properties in mice lacking *PRG4*. *Arthritis Rheum* 2010;62:1666–74.
- Cook JL, Kuroki K, Visco D, Pelletier JP, Schulz L, Lafebvre FP. The OARSI histopathology initiative: recommendations for histological assessments of osteoarthritis in the dog. *Osteoarthritis Cartilage* 2010;18 Suppl 3:S66–79.
- Kinross KM, Montgomery KG, Kleinschmidt M, Waring P, Iveta I, Tikoo A, et al. An activating *Pik3ca* mutation coupled with *Pten* loss is sufficient to initiate ovarian tumorigenesis in mice. *J Clin Invest* 2012;122:553–7.
- Hindson BJ, Ness KD, Masquelier DA, Belgrader P, Heredia NJ, Makarewicz AJ, et al. High-throughput droplet digital PCR system for absolute quantitation of DNA copy number. *Anal Chem* 2011;83:8604–10.

21. Ripoché D, Gout J, Pommier RM, Jaafar R, Zhang CX, Bartholin L, et al. Generation of a conditional mouse model to target *Acrv1b* disruption in adult tissues. *Genesis* 2013;51:120–7.
22. Neogi T, Zhang Y. Epidemiology of osteoarthritis. *Rheum Dis Clin North Am* 2013;39:1–19.
23. Hochberg MC, Yerges-Armstrong L, Yau M, Mitchell BD. Genetic epidemiology of osteoarthritis: recent developments and future directions. *Curr Opin Rheumatol* 2013;25:192–7.
24. Louboutin H, Debarge R, Richou J, Selmi TA, Donell ST, Neyret P, et al. Osteoarthritis in patients with anterior cruciate ligament rupture: a review of risk factors. *Knee* 2009;16:239–44.
25. Brown TD, Johnston RC, Saltzman CL, Marsh JL, Buckwalter JA. Posttraumatic osteoarthritis: a first estimate of incidence, prevalence, and burden of disease. *J Orthop Trauma* 2006;20:739–44.
26. Elsaid KA, Fleming BC, Oksendahl HL, Machan JT, Fadale PD, Hulstyn MJ, et al. Decreased lubricin concentrations and markers of joint inflammation in the synovial fluid of patients with anterior cruciate ligament injury. *Arthritis Rheum* 2008;58:1707–15.
27. Ruan MZ, Erez A, Guse K, Dawson B, Bertin T, Chen Y, et al. Proteoglycan 4 expression protects against the development of osteoarthritis. *Sci Transl Med* 2013;5:176ra34.
28. Buckley MR, Bergou AJ, Fouchard J, Bonassar LJ, Cohen I. High-resolution spatial mapping of shear properties in cartilage. *J Biomech* 2010;43:796–800.
29. Buckley MR, Gleghorn JP, Bonassar LJ, Cohen I. Mapping the depth dependence of shear properties in articular cartilage. *J Biomech* 2008;41:2430–7.
30. Wong BL, Bae WC, Gratz KR, Sah RL. Shear deformation kinematics during cartilage articulation: effect of lubrication, degeneration, and stress relaxation. *Mol Cell Biomech* 2008;5:197–206.
31. Hughes LC, Archer CW, ap Gwynn I. The ultrastructure of mouse articular cartilage: collagen orientation and implications for tissue functionality: a polarised light and scanning electron microscope study and review. *Eur Cell Mater* 2005;9:68–84.
32. Hashimoto S, Nishiyama T, Hayashi S, Fujishiro T, Takebe K, Kanzaki N, et al. Role of p53 in human chondrocyte apoptosis in response to shear strain. *Arthritis Rheum* 2009;60:2340–9.
33. Healy ZR, Lee NH, Gao X, Goldring MB, Talalay P, Kensler TW, et al. Divergent responses of chondrocytes and endothelial cells to shear stress: cross-talk among COX-2, the phase 2 response, and apoptosis. *Proc Natl Acad Sci U S A* 2005;102:14010–5.
34. Lee MS, Sun MT, Pang ST, Ueng SW, Chen SC, Hwang TL, et al. Evaluation of differentially expressed genes by shear stress in human osteoarthritic chondrocytes in vitro. *Chang Gung Med J* 2009;32:42–50.
35. Lee MS, Trindade MC, Ikenoue T, Goodman SB, Schurman DJ, Smith RL. Regulation of nitric oxide and bcl-2 expression by shear stress in human osteoarthritic chondrocytes in vitro. *J Cell Biochem* 2003;90:80–6.
36. Lee MS, Trindade MC, Ikenoue T, Schurman DJ, Goodman SB, Smith RL. Effects of shear stress on nitric oxide and matrix protein gene expression in human osteoarthritic chondrocytes in vitro. *J Orthop Res* 2002;20:556–61.
37. Ding L, Heying E, Nicholson N, Stroud NJ, Homandberg GA, Buckwalter JA, et al. Mechanical impact induces cartilage degradation via mitogen activated protein kinases. *Osteoarthritis Cartilage* 2010;18:1509–17.
38. Zhu F, Wang P, Kontogianni-Konstantopoulos A, Konstantopoulos K. Prostaglandin (PG)₂ and 15-deoxy- $\Delta^{12,14}$ -PGJ₂, but not PGE₂, mediate shear-induced chondrocyte apoptosis via protein kinase A-dependent regulation of polo-like kinases. *Cell Death Differ* 2010;17:1325–34.
39. Zhu F, Wang P, Lee NH, Goldring MB, Konstantopoulos K. Prolonged application of high fluid shear to chondrocytes recapitulates gene expression profiles associated with osteoarthritis. *PLoS One* 2010;5:e15174.
40. Waller KA, Zhang LX, Fleming BC, Jay GD. Preventing friction-induced chondrocyte apoptosis: comparison of human synovial fluid and hylan G-F 20. *J Rheumatol* 2012;39:1473–80.
41. Jay GD, Elsaid KA, Kelly KA, Anderson SC, Zhang L, Teeple E, et al. Prevention of cartilage degeneration and gait asymmetry by lubricin tribosupplementation in the rat following anterior cruciate ligament transection. *Arthritis Rheum* 2012;64:1162–71.
42. Jay GD, Fleming BC, Watkins BA, McHugh KA, Anderson SC, Zhang LX, et al. Prevention of cartilage degeneration and restoration of chondroprotection by lubricin tribosupplementation in the rat following anterior cruciate ligament transection. *Arthritis Rheum* 2010;62:2382–91.
43. Teeple E, Elsaid KA, Jay GD, Zhang L, Badger GJ, Akelman M, et al. Effects of supplemental intra-articular lubricin and hyaluronic acid on the progression of posttraumatic arthritis in the anterior cruciate ligament-deficient rat knee. *Am J Sports Med* 2011;39:164–72.
44. Flannery CR, Zollner R, Corcoran C, Jones AR, Root A, Rivera-Bermudez MA, et al. Prevention of cartilage degeneration in a rat model of osteoarthritis by intraarticular treatment with recombinant lubricin. *Arthritis Rheum* 2009;60:840–7.
45. Elsaid KA, Zhang L, Waller K, Tofte J, Teeple E, Fleming BC, et al. The impact of forced joint exercise on lubricin biosynthesis from articular cartilage following ACL transection and intra-articular lubricin's effect in exercised joints following ACL transection. *Osteoarthritis Cartilage* 2012;20:940–8.
46. Ai M, Cui Y, Sy MS, Lee DM, Zhang LX, Larson KM, et al. Anti-lubricin monoclonal antibodies created using lubricin-knockout mice immunodetect lubricin in several species and in patients with healthy and diseased joints. *PLoS One* 2015;10:e0116237.
47. Rai MF, Hashimoto S, Johnson EE, Janiszak KL, Fitzgerald J, Heber-Katz E, et al. Heritability of articular cartilage regeneration and its association with ear wound healing in mice. *Arthritis Rheum* 2012;64:2300–10.